Desalination and Water Treatment
www.deswater.com

doi: 10.5004/dwt.2020.24992

184 (2020) 139–149
April

PEI-modified chromium-based metal organic framework for Cr(VI) removal from aqueous solution

Zhuan-nian Liu, A-ping Fan*, Xiao-gang Han, Habiba Shapour, Qing-yun Zhang

College of Geology and Environment, Xi'an University of Science and Technology, Xi'an 710054, China, Tel. +86 18710722004; email: 511073824@qq.com (A. Fan), Tel. +86 13892803449; email: zhuannianliu@163.com (Z. Liu), Tel. +86 15961291337; email: 237414866@qq.com (X. Han), Tel. +86 13201761150; email: Habiba.shapour33@gmail.com (H. Shapour), Tel. +86 18802998912; email: 584471206@qq.com (Q. Zhang)

Received 26 March 2019; Accepted 30 September 2019

ABSTRACT

The chelating adsorbent PEI-MIL-101(Cr) was prepared by introducing polyethyleneimine (PEI) into the MIL-101(Cr) channel in this paper. X-ray diffractometer, Fourier transform infrared spectrometer and scanning electron microscope were applied to characterize the structure and morphology of MIL-101(Cr) and PEI-MIL-101(Cr). The adsorption properties and mechanism of the MIL-101(Cr) and PEI-MIL-101(Cr) to Cr(VI) were studied. The results showed that adsorption capacity of PEI-MIL-101(Cr) for Cr(VI) was obviously better than MIL-101(Cr). The adsorption isotherm of Cr(VI) onto MIL-101(Cr) and PEI-MIL-101(Cr) can be described by Langmuir model. The maximum adsorption amount for Cr(VI) onto MIL-101(Cr) and 30% PEI-MIL-101(Cr) was 61.99 and 40.34 mg/g. The adsorption kinetic data of the two adsorbents followed the pseudo second-order model. The negative values ΔH and ΔG illustrate that the process is spontaneous and exothermic. PEI-MIL-101(Cr) can be reused for four times.

Keywords: MOFs; MIL-101(Cr); Cr(VI); Polyethyleneimine (PEI); Adsorption

1. Introduction

Heavy metal ions are considered to be highly toxic low-density chemicals, which are persistent and non-biodegradable, accumulate easily in organisms, and have a serious impact on the ecological environment and human health [1]. Among many heavy metal ions, chromium is one of the most dangerous pollutants. The chromium and its compounds in wastewater mainly come from various industries including mining operations, metal processing, leather tanning, water cooling, pigment manufacturing, etc. [2]. Chromium exists in trivalent [Cr(III)] and hexavalent [Cr(VI)] oxidation states and Cr(VI) ($CrO_4^{2-}/Cr_2O_7^{2-}$ ions) is reported to be more mutagenic and carcinogenic beyond the 0.05 mg/L [3]. The tolerant limiting value of Cr(VI) in drinking water is 0.05 mg/L as suggested by World Health Organization [4]. The methods used to treat Cr(VI) in wastewater include adsorption [5], photocatalytic reduction [6], ion exchange [7], electrochemical reduction [8], etc. However, each method has their own disadvantages, for example, chemical reduction demands chemical additives and is followed by precipitation, electrochemical reduction, generates large amounts of sludge [9]. Photocatalytic reduction is limited by low photo conversion efficiency of photocatalyst [3,10]. Adsorption has been proposed as a promising technique for removal of metal ions from contaminated water for its wide source of adsorbents, low cost, good removal effect, and some adsorbents can be recycled [11,12].

Metal organic framework (MOF) materials also known as porous coordination polymers, which are a new class of porous

---

* Corresponding author.

crystal material, formed by coordination polymerization of inorganic metal ions or metal cluster units with multi-dentate organic ligands [13]. Comparing with other traditional porous materials MOFs have attracted considerable interests due to their uniform dispersion structure, large surface area, high porosity, open metal sites and functional modification [14]. Different kinds of MOFs can be prepared that have different functions by selection of different metal elements and organic ligands. More MOFs are reported to have MIL-n (MIL = Materials of Institut Lavoisier) series materials such as MIL-53(Al) [15], MIL-100(Fe) [16], MIL-101(Cr) [17], zinc-based material MOF-5 [18], cobalt-based material ZIF-8 (ZIF = zeolitic imidazolate frameworks) [19], copper-based material HKUST-1 [20]. The MOFs have been adopted for widespread applications including gas storage [21], gas adsorption or separation [22], catalysis [23], drug delivery [24] because of diversity of the MOFs types, structures and functions. In recent years, the adsorption treatment of pollutants in wastewater by MOFs has attracted more attention.

Chromium-based MOF material MIL-101(Cr) is a three-dimensional framework material with MTN (Mobil Thirty Nine) topology, which is formed by the connection of chromium trimer [$Cr_3O(CO_2)_6$] and terephthalic acid (H_2BDC) [25]. MIL-101(Cr) has acid and alkali resistance, larger surface area, excellent thermal stability, water and chemical stability, which has shown good effects in the adsorption treatment of wastewater [26]. MIL-101(Cr) has a metal active site, which can be modified by surface modification, immobilization of functional materials or synthesis of composite materials with suitable materials to improve its adsorption and removal of pollutants in wastewater. Luo et al. [27] prepared a thymine-functionalized MIL-101(Cr) material by post-synthesis method, its maximum adsorption amount to Hg^{2+} was 51.27 mg/g. Yang et al. [28] prepared the MoS_2/MIL-101(Cr) composite adsorbent by hydrothermal synthesis, and its adsorption amount of Rhodamine B was 344.8 mg/g. Luo et al. [27] synthesized the sulfonate-functionalized MIL-101(Cr) adsorbent with negative charge on its surface. The removal of cationic dyes methylene blue (MB) and malachite green (MG) in aqueous solution was better due to electrostatic attraction [29].

Polyethylenimine (PEI) is a typical water-soluble polymer polyamine consisting of a large number of amine groups on its macromolecular chains. It can strongly chelate heavy metal ions and has been used in the functionalization of traditional adsorbents and MOFs [30]. PEI-modified MOFs are mostly used for gas adsorption and separation, and there are few studies on the removal of pollutants in water. Xian et al. [31] used PEI-modified ZIF-8 material for CO_2/N_2 separation and adsorption of CO_2. The results showed that CO_2 adsorption capacity and CO_2/N_2 selectivity of PEI@ZIF-8 were 6.2 and 27 times that of ZIF-8, respectively. Fu et al. [32] prepared UiO-66/PEI material, the adsorption capacity of UiO-66 to CO_2 was 1.5 times that of UiO-66 and reached 3.13 mmol/g at 25°C. Lin et al. [33] synthesized MIL-101 with different PEI loadings and applied to adsorb CO_2. Although the surface area and pore volume of MIL-101 decreased with PEI loading, the adsorption capacity of composite material for CO_2 increased significantly. Quan et al. [34] found that the introduction of PEI changed the surface charge of Cu-BTC material and made the surface of the Cu-BTC have a positive charge, which is conducive to the adsorption of the anionic dye Congo Red.

In this paper, the chrome-based MOF MIL-101(Cr) was prepared by hydrothermal synthesis method. The chelating function adsorbent PEI-MIL-101(Cr) was prepared by modifying MIL-101(Cr) with polyethyleneimine (PEI) by post-modification. The adsorptive properties and mechanism for Cr(VI) adsorption onto MIL-101(Cr) and PEI-MIL-101(Cr) were investigated.

2. Experiment

2.1. Materials and instrumentation

2.1.1. Materials

The chromium(III) nitrate nonahydrate ($Cr(NO_3)_3{\cdot}9H_2O$), hydrofluoric acid (HF), terephthalic acid (H_2BDC), N, N-dimethylformamide (DMF) used in this study was purchased from Sino Pharm Chemical Reagent Co. Ltd., China. Polyethyleneimine was purchased from Shanghai Aladdin Biochemical Technology Co. Ltd., China. Potassium dichromate was purchased from Tianjin Tianhe Chemical Reagent Factory, China. All chemical agents used in this paper are analytical reagents and deionized water was used to prepare all solutions.

2.1.2. Instrumentation

The concentration of Cr(VI) was quantified by the diphenylcarbazide method on a ultraviolet-visible spectrophotometer (TU-1810SPC, Universal Analysis, Beijing) at 540 nm. The X-ray powder diffraction (XRD) analysis was performed using a XD-3 (Universal Analysis, Beijing) diffractometer with Cu-Kα radiation (40 kV, 40 mA, λ¼ 0.15418 nm) to identify the structure and the composition of the composite. The Fourier transform infrared (FT-IR) spectroscopy (550s, PerkinElmer, United States) is used to analyze the chemical structure of samples. N_2 adsorption apparatus, (ASAP 2020, Micromeritics, United States) was used to analyze the surface area and pore size distribution. The morphology analysis of samples was conducted by scanning electron microscope (SEM, JSM-6710F, JEOL, Japan).

2.2. Synthesis of MIL-101(Cr) and PEI-MIL-101(Cr)

MIL-101(Cr) was synthesized using the hydrothermal method [35]. $Cr(NO_3)_3{\cdot}9H_2O$ (4.0 g), terephthalic acid (1.6 g), 0.43 mL fluorhydric acid (40%) were dissolved in 48 mL deionized water and magnetically stirred for half of an hour. Then, ultrasound assisted for 30 min to mix the solution evenly. Subsequently, the solution was translated to a Teflon-lined stainless-steel autoclave of 100 mL capacity and placed at 220°C for 8 h. The green color sample was centrifuged separation after cooling to room temperature. The sample MIL-101(Cr) was washed and purified three times with N,N-dimethylformamide and alcohol at 60°C for 1 h, then washed several times with deionized water. The sample was dried overnight at 150°C in a vacuum drying chamber, and the purified MIL-101(Cr) sample was obtained.

The PEI-MIL-101(Cr) material was prepared by impregnation method. First, the MIL-101(Cr) was dried at 150°C for

12 h to remove the coordination water on the Cr site. Then the 0.02, 0.05, 0.09, 0.13 and 0.2 g PEI were dissolved in anhydrous methanol and stirred for 1 h. The 0.2 g MIL-101(Cr) material was separately added into the PEI/methanol solution, immersed overnight, stirred under reflux and dried under vacuum condition at 65°C to obtain the PEI-modified chromium-based MOF material, named 10% PEI-MIL-101(Cr), 20% PEI-MIL-101(Cr), 30% PEI- MIL-101(Cr), 40% PEI-MIL-101(Cr), 50% PEI-MIL-101(Cr).

2.3. Adsorption experiments

2.3.1. Influence of PEI ratio on adsorption performance

50 mg MIL-101(Cr) or different ratio of PEI-modified adsorbent PEI-MIL-101(Cr) was added into 100 mL (20 mg/L) of Cr(VI) solution, and shaken continuously for 3 h at 25°C. The samples were filtered, and then it was analyzed for the concentration of Cr(VI) remaining using a spectrophotometer.

2.3.2. Adsorption kinetics

50 mg MIL-101(Cr) or PEI-MIL-101(Cr) adsorbent was added into 100 mL (20 mg/L) of Cr(VI) solution, and shaken at 25°C. Samples were taken at different time intervals (10, 20, 30, 60, 90, 120, 180 and 240 min) and filtered, then analyzed for the Cr(VI) concentration in the solution.

2.3.3. Adsorption thermodynamics

In the equilibrium experiments, 50 mg MIL-101(Cr) or PEI-MIL-101(Cr) adsorbent was added into 100 mL (5, 10, 20, 30, 50 and 100 mg/L) of Cr(VI) solution, respectively, and shaken continuously for 3 h at 25°C. The samples were filtered, then the filtrates were analyzed for the Cr(VI) concentration remaining in the solution.

2.3.4. Influence of pH value, dosage and temperature on adsorption

A certain amount of MIL-101(Cr) or PEI-MIL-101(Cr) adsorbent was added into 100 mL (20 mg/L) of Cr(VI) solution, the different pH of each test solution was adjusted using 0.1 M NaOH and 0.1 M HCl solutions, and shaken continuously for 3 h at different temperature. The samples were filtered and the solution concentration of Cr(VI) was analyzed.

The amount of adsorption was determined by the following equation:

$$q_e = \frac{\left(C_0 - C_e\right)V}{m} \tag{1}$$

where q_e is the adsorption amount at equilibrium, mg/g; C_0 is the initial concentration of Cr(VI) in solution, mg/L; C_e is the final concentration of Cr(VI), mg/L; V is the volume of Cr(VI) solution, L; m is the mass of the adsorbent, g.

2.4. Desorption regeneration experiment

The adsorbed saturated adsorbent was washed three times with deionized water, then 100 mL (0.05 mol/L) NaOH was added to the solution and sonicated for 30 min; this process was repeated twice. The adsorbent was washed several times with deionized water until neutral and dried, repeating adsorption experiments were performed.

3. Results and discussion

3.1. Characterization of MOF materials

3.1.1. XRD analysis

The XRD patterns of MIL-101(Cr) and PEI-MIL-101(Cr) materials are presented in Fig. 1. As it can be seen from Fig. 1, the MIL-10(Cr) is showed obvious distinct peaks at 3.3°, 5.2°, 8.5° and 9.1°(2θ), which is consistent with the literature [36]. This indicated that MIL-101(Cr) was successfully synthesized and had a complete crystal form. Comparing PEI-MIL-101(Cr) modified with different proportions of polyethyleneimine shows that the diffraction peak of the material becomes weaker with the increasing of PEI addition ratio. When the ratio exceeds 40%, the diffraction peak is obviously weakened, it indicated that the crystal structure changes, which may be due to the fact that the introduction of PEI slightly occupies the pores of material and crystallinity of the material decreases.

3.1.2. FT-IR spectra analysis

The FT-IR spectra of the MIL-101(Cr) and 30% PEI-MIL-101(Cr) materials are shown in Fig. 2. In the infrared spectrum of MIL-101(Cr), the peak at 1,700 cm^{-1} is stretching vibration peak of the C=O double bond in the –COOH of unreacted terephthalic acid [37]. While the peaks at 1,626 cm^{-1} indicates the presence of a corresponding amount of water molecules in the adsorbent. The antisymmetric stretching vibration and the symmetric stretching vibration peak of the carboxyl group at 1,539 and 1,393 cm^{-1} is clearly shown in the spectra [38]. The bands observed between 600 and 1,600 cm^{-1} are attributed to phenyl groups which primarily incorporate the C=C tensile vibration peak at 1,508 cm^{-1}, and the bending vibration peak of the C–H bond

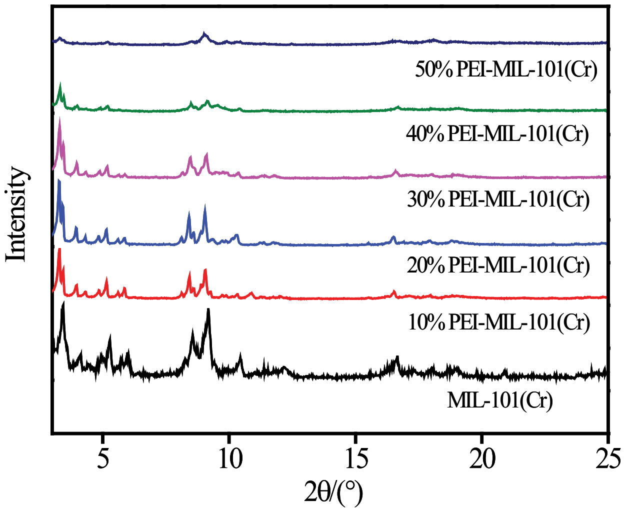

Fig. 1. XRD patterns of MIL-101(Cr) and PEI-MIL-101(Cr).

deformation at 1,159; 1,018; 885 and 751 cm^{-1}. The absorption peak at 578 cm^{-1} corresponds to the stretching vibration of the Cr–O bond [39]. The appearances of these peaks indicate that MIL-101(Cr) has been successfully synthesized.

In the infrared spectrum of PEI-MIL-101(Cr), the peak at 3,485 cm^{-1} correspond to the stretching vibrations of the absorption peak of –NH, while the peaks at 2,922 and 2,853 cm^{-1} are, respectively, believed to the asymmetric and symmetric stretching vibration peaks of the C–H bond of methylene groups (–CH_2–) in the PEI molecule. The peak at 1,700 cm^{-1} disappeared because the introduction of amino group neutralized the carboxyl group in MIL-101(Cr). In addition, the peak at 1,563 cm^{-1} was caused by the in-plane bending vibration peak of N–H bond, the peak at 921 cm^{-1} is the bending vibration absorption peak of C–N bond, and 657 cm^{-1} is the bending vibration absorption peak of primary amine –NH. The appearances of these peaks indicate that polyethyleneimine was successfully introduced into the MIL-101(Cr) material structure.

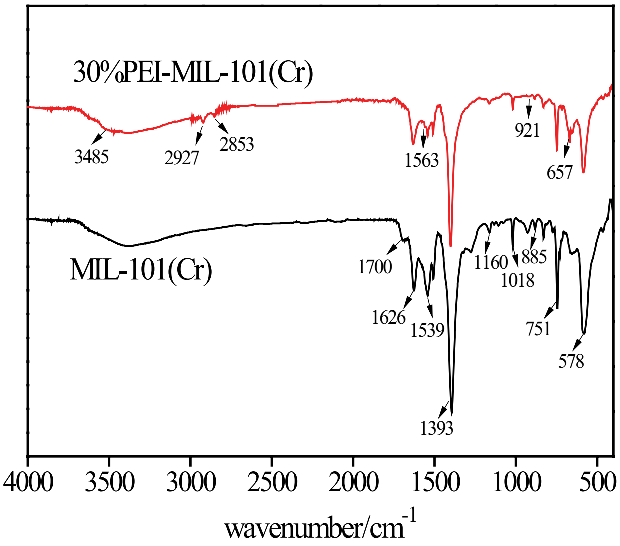

Fig. 2. FT-IR spectra of MIL-101(Cr) and 30% PEI-MIL-101(Cr).

3.1.3. SEM analysis

The SEM images of MIL-101(Cr) and PEI-MIL-101(Cr) materials are presented in Fig. 3. Figs. 3a and b are SEM photographs of MIL-101(Cr), Figs. 3c and d are SEM photographs of 30% PEI-MIL-101(Cr). It can be seen from Figs. 3a and b that the octahedral-shaped crystals characteristic of the MIL-101(Cr) lattice are evident. The MIL-101(Cr) materials have good crystal formability, smooth surface and relatively uniform particles, which is consistent with the structure of MIL-101(Cr) material reported in the literature [40]. It can be seen from Figs. 3c and d that the material modified by polyethyleneimine still maintains the octahedral structure, but the regularity and integrity of the crystal morphology decreased slightly. The introduction of PEI has a slight effect on the structure of MIL-101(Cr), the surface of the modified

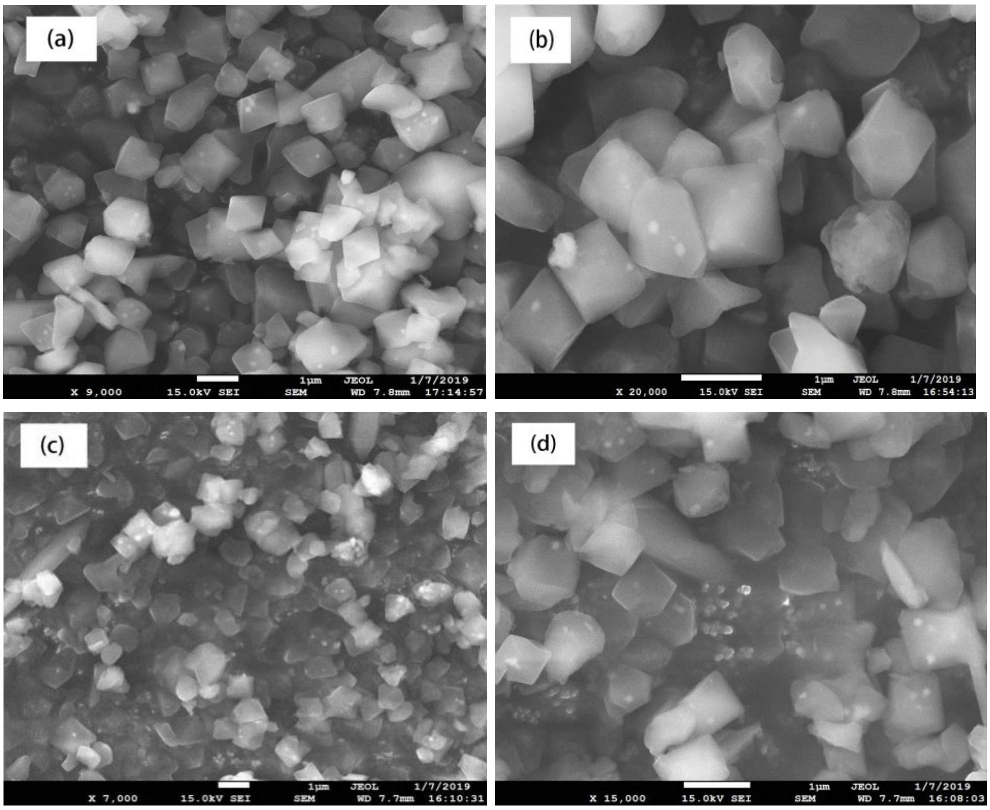

Fig. 3. SEM analysis of (a,b) MIL-101(Cr) and (c,d) 30% PEI-MIL-101(Cr).

material is rougher, which is more conducive to the adsorption of pollutants [41].

3.1.4. BET surface areas and pore structure analysis

The nitrogen adsorption–desorption isotherms and pore size distributions of MIL-101(Cr) and 30% PEI-MIL-101(Cr) are given in Figs. 4 and 5. It can be seen from Fig. 4 that MIL-101(Cr) shows a very high N_2 saturated adsorption capacity, and the N_2 saturated adsorption amount onto 30% PEI-MIL-101(Cr) drops obviously. As can be seen from Fig. 5 that the pore volume and pore size of 30% PEI-MIL-101(Cr) is significantly smaller than MIL-101(Cr). The data of surface area and pore structure parameters of MIL-101(Cr) and 30% PEI-MIL-101(Cr) are listed in Table 1. It can be seen from the table that the specific surface area and pore volume of 30% PEI-MIL-101(Cr) are lower than MIL-101(Cr), because the introduction of PEI occupies a larger pore size of MIL-101(Cr), lead to the specific surface area and pore volume of 30% PEI-MIL-101(Cr) decrease. But it is found that the pore diameter of MIL-101(Cr) is slightly smaller than 30% PEI-MIL-101(Cr), this illustrates that the pore structure has not changed obviously after PEI is induced.

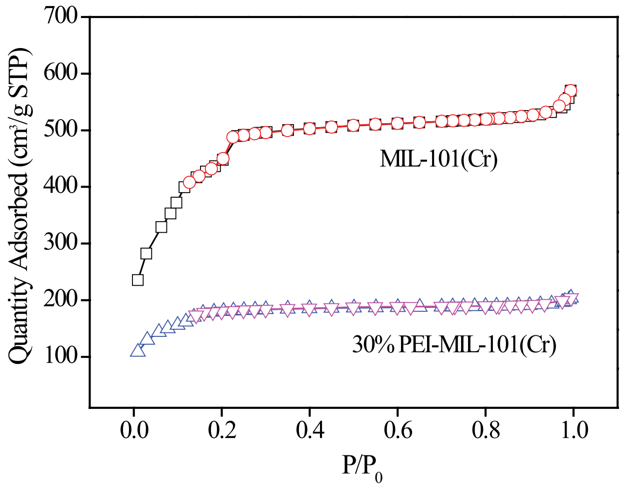

Fig. 4. Nitrogen isotherms analysis of MIL-101(Cr) and 30% PEI-MIL-101(Cr).

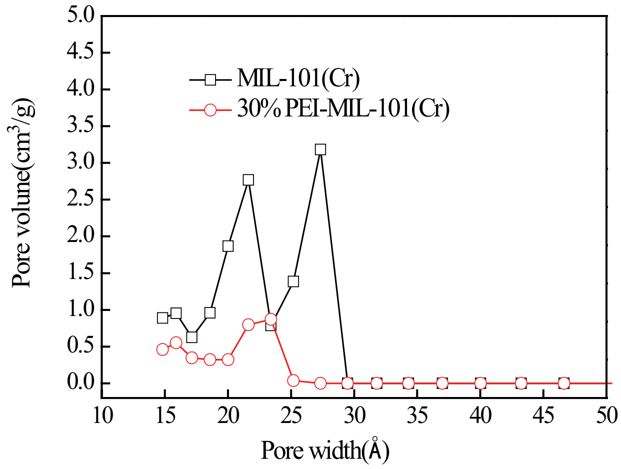

Fig. 5. Pore size distributions analysis of MIL-101(Cr) and 30% PEI-MIL-101(Cr).

3.2. Effect of PEI ratio on adsorption performance

The adsorption effect of MIL-101(Cr) and different ratios of PEI-modified PEI-MIL-101(Cr) adsorbent on Cr(VI) are shown in Fig. 6. It can be seen clearly from the figure that adsorption amount of Cr(VI) onto PEI-modified MIL-101(Cr) is improved significantly. The 30% PEI-MIL-101(Cr) has the best modification effect, thus the adsorption amount of Cr(VI) is added up to 31.45 mg/g. As the proportion of PEI increases, the adsorption amount of Cr(VI) decreases. This result is due to the fact that the crystal structure of the material is changed due to excessive PEI, MIL-101(Cr) partial channel collapse and pore reduction. In the subsequent experiments, the adsorption performance and mechanism of Cr(VI) were investigated by 30% PEI-MIL-101(Cr) adsorbent.

3.3. Adsorption kinetics

The effects of time on the adsorption properties of MIL-101(Cr) and PEI-MIL-101(Cr) are presented in Fig. 7. It can be seen from the figure that the adsorption amount of MIL-101(Cr) and PEI-MIL-101(Cr) adsorbents for Cr(VI) increased rapidly before 30 min. It is due to that MIL-101(Cr) and PEI-MIL-101(Cr) have a large specific surface area, microporous

Table 1
Surface area and pore structure parameters of MIL-101(Cr) and 30% PEI-MIL-101(Cr)

Samples	BET surface area (m^2/g)	Pore volume (cm^3/g)	Pore diameter (nm)
MIL-101(Cr)	1,654.70	0.86	2.08
30% PEI-MIL-101(Cr)	651.91	0.31	1.91

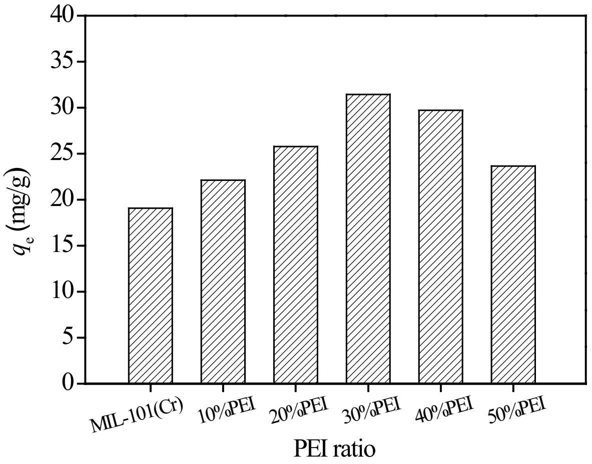

Fig. 6. Effect of PEI ratio on adsorption of Cr(VI) onto MIL-101(Cr) and PEI-MIL-101(Cr).

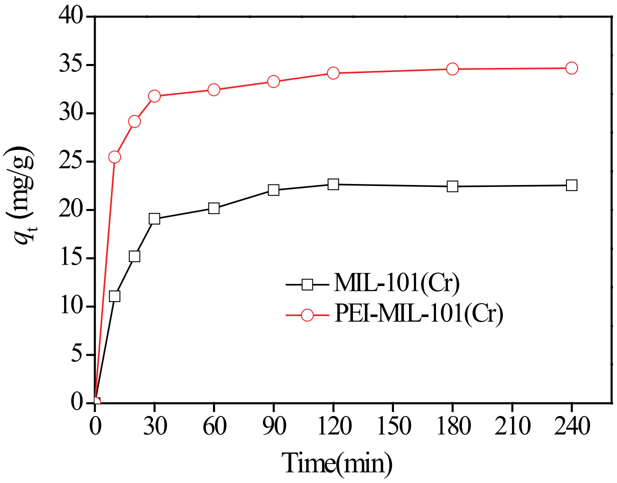

Fig. 7. Effect of time on the adsorption of Cr(VI) onto MIL-101(Cr) and 30% PEI-MIL-101(Cr).

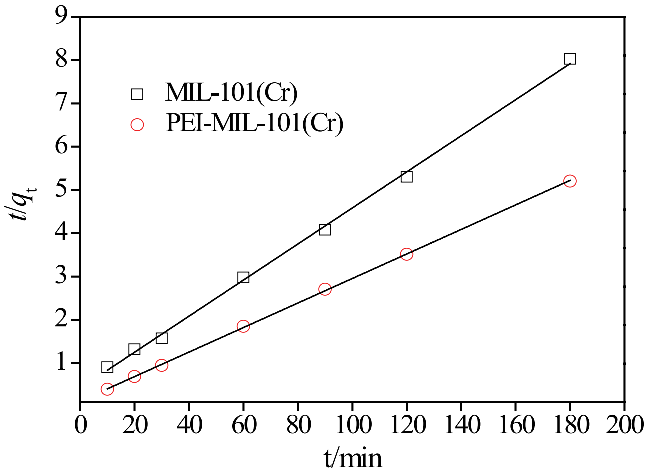

Fig. 8. Pseudo second-order kinetic curves for Cr(VI) adsorption onto MIL-101(Cr) and 30% PEI-MIL-101(Cr).

and mesoporous structures, a large number of active adsorption sites on the surface [42]. With the increasing of time, most of the adsorption active sites were gradually occupied, and the adsorption rate slowed down until it finally reaches equilibrium about 180 min. The adsorption capacity for Cr(VI) onto 30% PEI-MIL-101(Cr) increased 54% than MIL-101(Cr). The reason is amine chelating groups which are introduced into the PEI-MIL-101(Cr) for Cr(VI) [43].

In order to better study the relationship between the adsorption process of Cr(VI) by MIL-101(Cr) and PEI-MIL-101(Cr) and time, the kinetics of Cr(VI) adsorption can be analyzed using the Lagergren first-order reaction kinetics model and the pseudo second-order kinetics model to determine the adsorption rate constants. A linear form of the Lagergren first-order model is expressed as follows [44]:

$$\log(q_e - q_t) = \log q_e - \frac{k_1}{2.303}t \tag{2}$$

where q_e and q_t (mg/g), are the amounts adsorbed at equilibrium and at time t (min), respectively, and k_1 (min^{-1}) is the rate constant for the Lagergren first-order model, the kinetic data are further analyzed using pseudo second-order kinetics expressed as follows [45]:

$$\frac{t}{q_t} = \frac{1}{k_2 q_e^2} + \frac{1}{q_e}t \tag{3}$$

where k_2 (g/mg min) is the rate constant of the pseudo second-order model.

The pseudo second-order plots for Cr(VI) adsorption onto the MIL-101(Cr) and 30% PEI-MIL-101(Cr) are presented in Fig. 8. The kinetic parameters obtained for the Lagergren first-order and the pseudo second-order models are presented in Table 2 (where $q_{e,c}$ is the calculated equilibrium adsorption amount). As it is seen in Table 2, the regression correlation coefficients (R^2) of Cr(VI) adsorption onto MIL-101(Cr) and PEI-MIL-101(Cr) adsorbents for the pseudo second-order kinetic model are all greater than the R^2 for the Lagergren first-order kinetic model, and the linear correlation coefficient R^2 is 0.9986 and 0.9998, respectively. The data for adsorbed amounts calculated at equilibrium from the pseudo second-order kinetics ($q_{e,c}$) are also close to the amounts adsorbed at equilibrium in the experiments. The initial concentration of Cr(VI) is 20 mg/L in this experiment, the results agree with the Azizian's [46] conclusion that the adsorption process obeys pseudo-first-order kinetics at high initial concentration of solute, while it obeys pseudo-second-order kinetics model at lower initial concentration of solute.

3.4. Adsorption isotherm

The adsorption isotherms for Cr(VI) adsorption onto MIL-101(Cr) and PEI-MIL-101(Cr) adsorbents are given in Fig. 9. It can be seen from Fig. 9 that the adsorption capacity of Cr(VI) on 30% PEI-MIL-101(Cr) is significantly higher than that of MIL-101(Cr). The experimental data were fitted using the Langmuir and Freundlich adsorption isotherm equations.

Table 2
Kinetic model parameters for Cr(VI) adsorption onto MIL-101(Cr) and 30% PEI-MIL-101(Cr)

Adsorbents	q_e (mg/g)	Lagergren first-order			Pseudo second-order		
		k_1 (min^{-1})	$q_{e,c}$ (mg/g)	R^2	k_2 (g/mg min)	$q_{e,c}$ (mg/g)	R^2
MIL-101(Cr)	22.43	0.0246	14.15	0.9660	0.0042	23.98	0.9986
30% PEI-MIL-101(Cr)	34.58	0.0364	29.47	0.9682	0.0066	35.34	0.9998

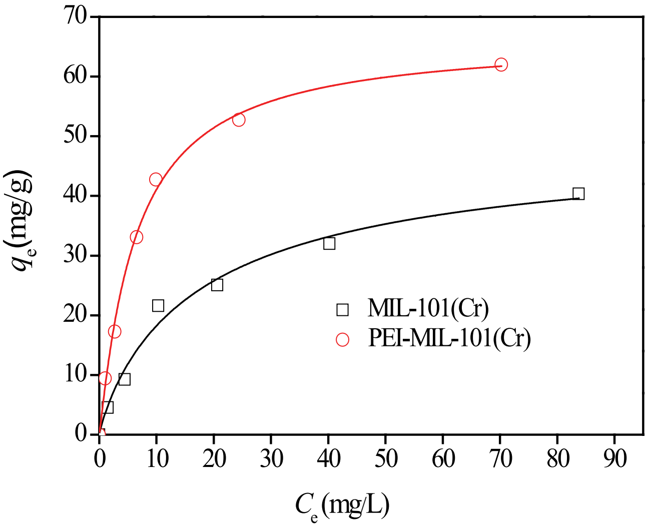

Fig. 9. Adsorption isotherms for Cr(VI) onto MIL-101(Cr) and PEI-MIL-101(Cr) at 298 K.

The Langmuir adsorption isotherm model is given as follows [47]:

$$\frac{1}{q_e} = \frac{1}{Q^0} + \left(\frac{1}{bQ^0}\right)\left(\frac{1}{C_e}\right) \tag{4}$$

where Q^0 is the amount of monomolecular layer saturated adsorption (mg/g); b is the Langmuir equilibrium constant. Q^0 and b can be calculated from the slope and intercept of the straight-line plot of $1/q_e$ vs. $1/C_e$.

The Freundlich adsorption isotherm model is represented as follows [48]:

$$\log q_e = \log K_F + \frac{1}{n}\log C_e \tag{5}$$

where K_F and n are adsorption constants related to temperature and adsorbent's specific surface area, which can be determined from the linear plot of log q_e vs. logC_e.

The data of adsorption for Cr(VI) onto MIL-101(Cr) and 30% PEI-MIL-101(Cr) adsorbents were fitted by Langmuir and Freundlich isotherm adsorption models, respectively. The fitting results are shown in Fig. 10 and Table 3. As it can be seen from the table that the regression correlation coefficients of Langmuir isotherm are 0.9866 and 0.9896 for MIL-101(Cr) and 30% PEI-MIL-101(Cr) adsorbents, respectively, which are larger than the Freundlich adsorption isotherm equation, suggesting that the Langmuir isotherm is applicable for describing Cr(VI) adsorption equilibrium. It is indicated that the adsorption for Cr(VI) onto the adsorbent is monolayer adsorption. The maximum adsorption capacity of Cr(VI) onto MIL-101(Cr) and 30% PEI-MIL-101(Cr) is 61.99 and 40.34 mg/g in this experiments. Comparison of Cr(VI) adsorption using various adsorbents is given in Table 4.

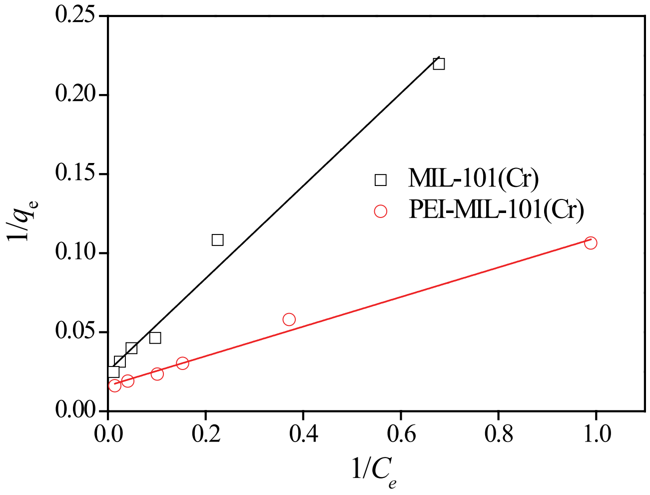

Fig. 10. Langmuir isotherms for Cr(VI) onto MIL-101(Cr) and 30% PEI-MIL-101(Cr).

3.5. Effect of pH values on adsorption

The effects of pH on the adsorption of Cr(VI) onto MIL-101(Cr) and 30% PEI-MIL-101(Cr) are shown in Fig. 11. It can be seen from Fig. 11 that the adsorption amount of Cr(VI) on MIL-101(Cr) and 30% PEI-MIL-101(Cr) increased with an increase in the pH range of 2.0–6.0 and 2.0–4.0, respectively. A further increase in pH led to a decline in the Cr(VI) adsorption. The pH_{PZC} was approximately 4.4 for MIL-101(Cr), the adsorbent surface is charged positively in the solution with pH below 4.4 and negatively above 4.4 [54]. The Cr(VI) exists in various forms in aqueous solution, such as $Cr_2O_7^{2-}$, $HCrO_4^-$ and CrO_4^{2-}. In pH range of 2.0–6.0 different forms of chromium ions, that is, $Cr_2O_7^{2-}$, $HCrO_4^-$ coexist and $HCrO_4^-$ dominates all these species. As the pH increased, $HCrO_4^-$ was converted into CrO_4^{2-} and $Cr_2O_7^{2-}$ species [3]. The surface charge of MIL-101(Cr) shows the positive charge at low pH, results in strong electrostatic attraction between positively charged adsorbent surface and chromate ions. With the increasing of pH, the adsorbent surface is charged

Table 3
Isotherm parameters of Cr(VI) adsorption onto MIL-101(Cr) and 30% PEI-MIL-101(Cr) (298 K)

Adsorbents	Langmuir			Freundlich		
	Q^0 (mg/g)	b (L/mg)	R^2	K_F	n	R^2
MIL-101(Cr)	39.53	0.086	0.9866	4.32	1.83	0.9463
PEI-MIL-101(Cr)	62.11	0.172	0.9896	11.53	2.19	0.9143

Table 4
Comparison of Cr(VI) adsorption using various adsorbents

No.	Adsorbents	Adsorption capability (mg/g)	Reference
1	Mango kernel bio-composite	322.58	[3]
2	Modified magnetic chitosan	153.85	[4]
3	Sulfuric acid modified leaves	170.8	[5]
4	Hexadecyl trimethyl ammonium bromide modified leaves	137.9	[5]
5	Tannin-hexamethylenediamine	283.29	[49]
6	Fe-Mg-type hydrotalcite	9.30	[50]
7	MnUiO-66	32.77	[51]
8	Nitrilotriacetic acid modified bamboo charcoal	270.00	[52]
9	Modified graphene oxide	300.88	[53]
10	30% PEI-MIL-101(Cr)	61.99	Present study

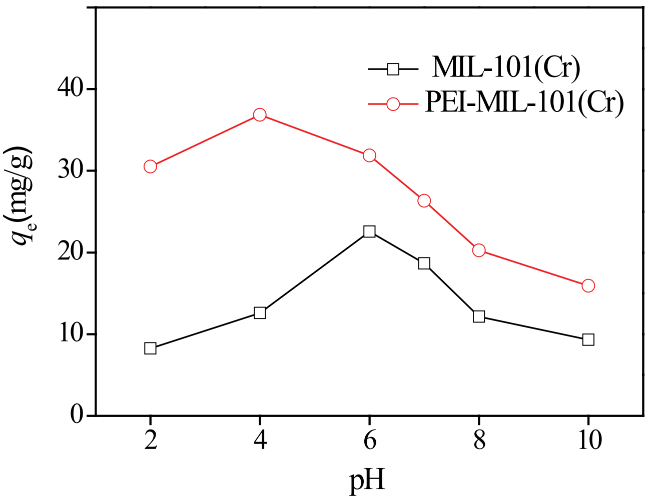

Fig. 11. Effect of pH on adsorption of Cr(VI) onto MIL-101(Cr) and 30% PEI-MIL-101(Cr).

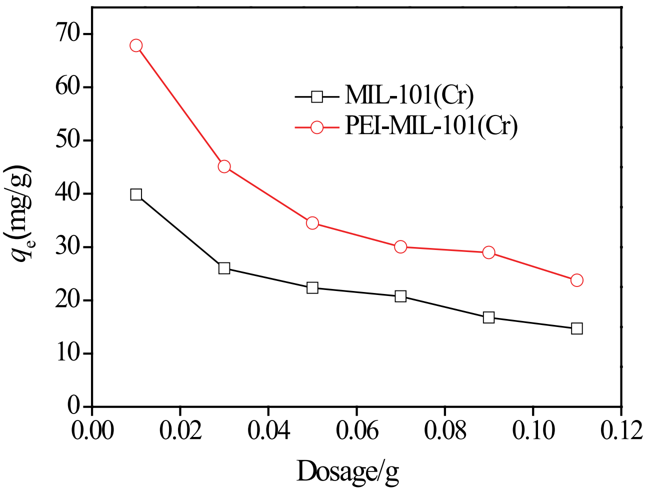

Fig. 12. Effect of dosage on the adsorption of Cr(VI) onto MIL-101(Cr) and 30% PEI-MIL-101(Cr).

negatively, the adsorption amount reduced due to repulsive forces increase between $Cr_2O_7^{2-}$ ions and adsorbents. The maximum adsorption capacity of the MIL-101(Cr) was appeared at pH 6.0. While, PEI is a cationic polymer, the protonation of the $-NH_2$ group in 30% PEI-MIL-101(Cr) produces $-NH_3^+$, which enhance the positive charge of the adsorbent surface and lead to the maximum adsorption capacity of PEI-MIL-101(Cr) for Cr(VI) was appeared at pH 4.0.

3.6. Effect of dosage on adsorption

The effects of dosage on adsorption for Cr(VI) onto MIL-101(Cr) and 30% PEI-MIL-101(Cr) are shown in Fig. 12. As seen from the figure that the equilibrium adsorption amount of Cr(VI) onto MIL-101(Cr) and 30% PEI-MIL-101(Cr) decreased with the increasing of dosage. The reason is the surface area and active sites increase with the increasing of dosage. However, the content of Cr(VI) in the solution is limited, the amount of adsorbed matter is unchanged, and the adsorption amount per unit mass of adsorbent decreases with the increase of dosage.

3.7. Effect of temperature on adsorption

The adsorption capacities of Cr(VI) onto MIL-101(Cr) and 30% PEI-MIL-101(Cr) at different temperatures are shown in Fig. 13. It can be seen from the figure that the adsorption capacities of Cr(VI) on MIL-101(Cr) and 30% PEI-MIL-101(Cr) decreased slightly with temperature increasing.

The related thermodynamic parameters for Cr(VI) adsorption onto 30% PEI-MIL-101(Cr) can be calculated from the following equation [54]:

$$\Delta G = \Delta H - T\Delta S \tag{6}$$

$$K_d = \frac{Q_e}{C_e} \tag{7}$$

$$\log K_d = \frac{\Delta S}{R} - \frac{\Delta H}{2.303RT} \tag{8}$$

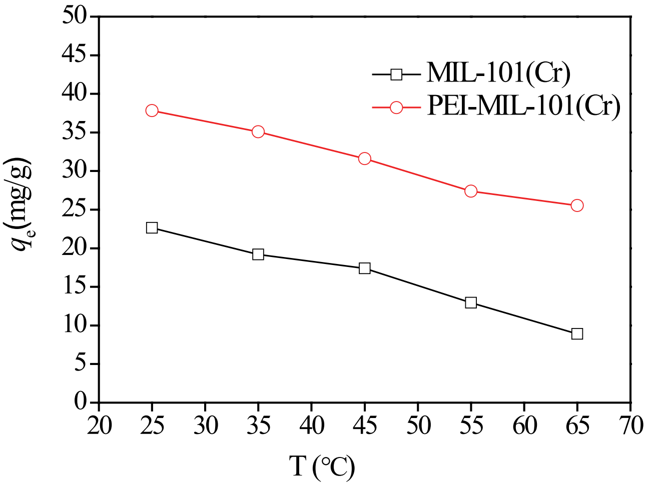

Fig. 13. Effect of temperature on the adsorption of Cr(VI).

where ΔG is the change in Gibbs free energy (J/mol); ΔH is the change in apparent enthalpy (J/mol); ΔS is the change in entropy (J/K mol); T is the thermodynamic temperature of reaction (K); and R is the universal gas constant, 8.314 (J K/mol); K_d is the partition coefficient; the parameters Q_e and C_e are the equilibrium concentrations of metal ions on the adsorbent (mg/g) and in the solution (mg/L), respectively.

Thermodynamic parameters determined from the plot are summarized in Table 5. The obtained negative values of ΔG° at all temperatures show that the adsorption process is spontaneous and feasible. The positive values of ΔH° indicate that the adsorption process is endothermic in nature.

The thermodynamics parameters obtained are listed in Table 5. The obtained negative value of ΔH (–25.66 kJ/mol) of the 30% PEI-MIL-101(Cr) for Cr(VI) confirmed that the adsorption process is exothermic in nature. The negative values of ΔG at different temperatures indicate that adsorption process is spontaneous. The negative value of ΔS (–30.26J/(mol K)) for 30% PEI-MIL-101(Cr) indicated that the adsorption occurred through the formation of an activated complex, suggesting that the Cr(VI) adsorption on the surface had an associated mechanism [55].

3.8. Reusability of adsorbent

The results of desorption regeneration experiments of MIL-101(Cr) and PEI-MIL-101(Cr) adsorbents are shown in Fig. 14. It can be seen from Fig. 14 that after four adsorption cycles, the adsorption amount of MIL-101(Cr) adsorbent for Cr(VI) decreased from 21.93 to 13.75 mg/g, and the adsorption amount of PEI-MIL-101(Cr) adsorbent for Cr(VI) decreased from 37.02 to 29.49 mg/g. After four cycles of reuse, MIL-101(Cr) and PEI-MIL-101(Cr) adsorbents still maintain good adsorption properties for Cr(VI).

Table 5
Thermodynamic parameters for Cr(VI) adsorption onto PEI-MIL-101(Cr)

T/K	ΔG/(kJ/mol)	ΔH/(kJ/mol)	ΔS/(J/K mol))	R^2
298	–34.68	–25.66	–30.26	0.975
308	–34.98			
318	–35.29			
328	–35.59			
338	–35.89			

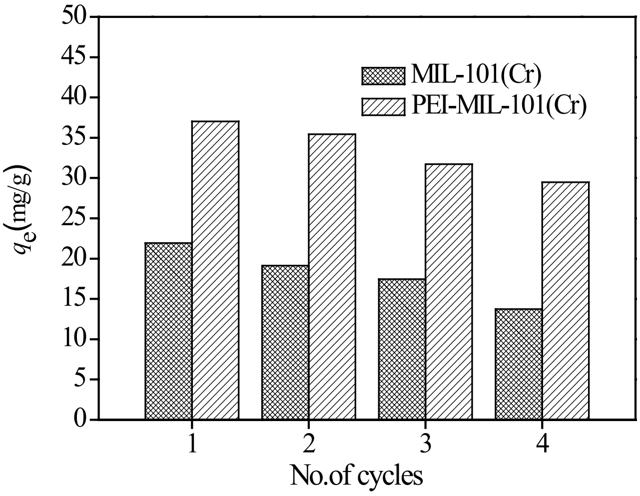

Fig. 14. Results of desorption regeneration of adsorbents.

4. Conclusions

In this paper, PEI-MIL-101(Cr) was prepared by modification with polyethyleneimine. PEI-MIL-101(Cr) material still maintains octahedral structure, but the introduction of polyethyleneimine effected the structure of MIL-101(Cr). The maximum adsorption amounts for Cr(VI) onto MIL-101(Cr) and 30% PEI-MIL-101(Cr) were 61.99 and 40.34 mg/g. The adsorption process of Cr(VI) onto MIL-101(Cr) and 30% PEI-MIL-101(Cr) follows the Langmuir isotherm. The adsorption kinetics follows the pseudo second-order kinetics, and the adsorption process is exothermic and spontaneous. 30% PEI-MIL-101(Cr) can be reused four times. This study suggested that PEI-MIL-101(Cr) is a promising material for heavy metal ions removal. It is an effective method to promote the selectivity and extend the application field by inducing functional groups into MIL-101(Cr).

References

[1] M. Cegłowski, B. Gierczyk, M. Frankowski, P. Łukasz, A new low-cost polymeric adsorbents with polyamine chelating groups for efficient removal of heavy metal ions from water solutions, React. Funct. Polym., 131 (2018) 64–74.
[2] J.B. Zhou, P.X. Wu, Z. Dang, N.W. Zhu, P. Li, J.H. Wu, X.D. Wang. Polymeric Fe/Zr pillared montmorillonite for the removal of Cr(VI) from aqueous solutions, Chem. Eng. J., 162 (2010) 1035–1044.
[3] M. Akram, H.N. Bhatti, M. Iqbal, S. Noreen, S. Sadaf, Biocomposite efficiency for Cr(VI) adsorption: kinetic, equilibrium and thermodynamics studies, J. Environ. Chem. Eng., 5 (2017) 400–411.
[4] C. Zheng, H. Zheng, Y. Wang, Y. Wang, W. Qu, Q An, Y. Liu, Synthesis of novel modified magnetic chitosan particles and their adsorption performance toward Cr(VI), Bioresour. Technol., 267 (2018) 1–8.

[5] Y. Zhang, M. Li, J. Li, Y. Yang, X. Liu, Surface modified leaves with high efficiency for the removal of aqueous Cr(VI), Appl. Surf. Sci., 484 (2019) 189–196.

[6] I. Kretschmer, A.M. Senn, J.M. Meichtry, G. Custo, E.B. Halac, R. Dillert, D.W. Bahnemann, M.I. Litter, Photocatalytic reduction of Cr(VI) on hematite nanoparticles in the presence of oxalate and citrate, Appl. Catal., B, 242 (2019) 218–226.

[7] Z. Ye, X. Yin, L. Chen, X. He, Z. Lin, C. Liu, S. Ning, X. Wang, Y. Wei, An integrated process for removal and recovery of Cr(VI) from electroplating wastewater by ion exchange and reduction-precipitation based on a silica-supported pyridine resin, J. Cleaner Prod., 236 (2019) 117631.

[8] X. Yang, L. Liu, M. Zhang, W. Tan, G. Qiu, L. Zheng, Improved removal capacity of magnetite for Cr(VI) by electrochemical Reduction, J. Hazard. Mater., 374 (2019) 26–34.

[9] W. Jin, H. Du, S. Zheng, Y. Zhang, Electrochemical processes for the environmental remediation of toxic Cr(VI): a review, Electorchim. Acta, 191 (2016) 1044–1055.

[10] N. Song, M. Zhang, H. Zhou, C. Li, G. Liu, S. Zhong, S. Zhang, Synthesis and properties of Bi_2WO_6 coupled with SnO_2 nano-microspheres for improved photocatalytic reduction of Cr^{6+} under visible light irradiation, Appl. Surf. Sci., (2018). https://doi.org/10.1016/j.apsusc.2019.143551.

[11] A. Kausar, G. MacKinnon, A. Alharthi, J. Hargreaves, H. N. Bhatti, M. Iqbal, A green approach for the removal of Sr(II) from aqueous media: kinetics, isotherms and thermodynamic studies, J. Mol. Liq., 257 (2018) 164–172.

[12] A. Kausar, H. N. Bhatti, M. Iqbal, A. Ashraf, Batch versus column modes for the adsorption of radioactive metal onto rice husk waste: conditions optimization through response surface methodology, Water Sci. Technol., 76 (2018) 1035–1043.

[13] L.Wang, Y.Z. Han, X. Feng, J.W. Zhou, P.F. Qi, B. Wang, Metal-organic frameworks for energy storage: batteries and supercapacitors, Coord. Chem. Rev., 307 (2016) 361–381.

[14] M.H. Yap, K.L. Fow, G.Z. Chen, Synthesis and applications of MOF-derived porous nanostructures, Green Energy Environ., 2 (2017) 218–245.

[15] A.L. Tarasov, V.I. Isaeva, O.P. Tkachenko, V. Chernyshev, Conversion of CO_2 into liquid hydrocarbons in the presence of a Cocontaining catalyst based on the microporous metal-organic framework MIL-53(Al), Fuel. Process. Technol., 176 (2018) 101–106.

[16] H.U. Rasheed, X.M. Lv, S.Y. Zhang, W. Wei, N. Ullah, J.M. Xie, Ternary MIL-100(Fe)@Fe_3O_4/CA magnetic nanophotocatalysts (MNPCs): Magnetically separable and Fenton-like degradation of tetracycline hydrochloride, Adv. Powder Technol., 29 (2018) 3305–3314.

[17] P.A. Konik, E.A. Berdonosova, I.M. Savvotin, S.N. Klyamkin, The influence of amide solvents on gas sorption properties of metal-organic frameworks MIL-101 and ZIF-8, Microporous Mesoporous Mater., 277 (2019) 132–135.

[18] F.A. Kloutse, A. Hourri, S. Natarajan, P. Benard, R. Chahine, Experimental benchmark data of CH_4,CO_2 and N_2 binary and ternary mixtures adsorption on MOF-5, Sep. Purif. Technol., 197 (2018) 228–236.

[19] N. Li, L. Zhou, X.Y. Jin, G. Owens, Z.L. Chen, Simultaneous removal of tetracycline and oxytetracycline antibiotics from wastewater using a ZIF-8 metal organic-framework, J. Hazard. Mater., 366 (2018) 563–572.

[20] M.R. Azhar, H.R. Abid, H.Q. Sun, V. Periasamy, M.O. Tadé, S.B. Wang, One-pot synthesis of binary metal organic frameworks (HKUST-1 and UiO-66) for enhanced adsorptive removal of water contaminants, J. Colloid. Interface Sci., 490 (2017) 685–694.

[21] K.K. Gangu, S. Maddila, S. B. Mukkamala, S. B. Jonnalagadda, Characteristics of MOF, MWCNT and graphene containing materials for hydrogen storage: a review, J. Energy Chem., 30 (2019) 132–144.

[22] K.M.C. Santos, R.J.O. Santos, M.M.D.A. Alves, J.F.D. Conto, G.R. Borges, C. Dariva, S.M. Egues, C.C. Santana, E. Franceschi, Effect of high pressure CO_2 sorption on the stability of metalorganic framework MOF-177 at different temperatures, J. Solid State Chem., 269 (2019) 320–327.

[23] Y.M. Zhang, X.Y. Yang, H.C. Zhou, Synthesis of MOFs for heterogeneous catalysis via linker design, Polyhedron, 154 (2018) 189–201.

[24] M. Pander, A. Żelichowska, W. Bury, Probing mesoporous Zr-MOF as drug delivery system for carboxylate functionalized molecules, Polyhedron, 156 (2018) 131–137.

[25] S. Karmakar, D. Roy, C. Janiak, S. De, Insights into multi-component adsorption of reactive dyes on MIL-101-Cr metal organic framework: experimental and modeling approach, Sep. Purif. Technol., 215 (2019) 259–275.

[26] S.J. Zhao, J. Mei, H.M. Xu, W. Liu, Z. Qu, Y. Cui, N.Q. Yan, Research of mercury removal from sintering flue gas of iron and steel by the open metal site of Mil-101(Cr), J. Hazard. Mater., 351 (2018) 301–307.

[27] X.B. Luo, T.T. Shen, L. Ding, W.P. Zhong, J.F. Luo, J.F. Luo, Novel thymine-functionalized MIL-101 prepared by post-synthesis and enhanced removal of Hg^{2+} from water, J. Hazard. Mater., 306 (2016) 313–322.

[28] C. Yang, J.H. Cheng, Y.C. Chen, Y.Y. Hu, Enhanced adsorption performance of MoS_2 nanosheet-coated MIL-101 hybrids for the removal of aqueous rhodamine B, J. Colloid. Interface. Sci., 504 (2017) 39–47.

[29] X.P. Luo, S.Y. Fu, Y.M. Du, J.Z. Guo, B. Li, Adsorption of methylene blue and malachite green from aqueous solution by sulfonic acid group modified MIL-101, Microporous Mesoporous Mater., 237 (2017) 268–274.

[30] Z.N. Liu, Y.Y. Liu, C.H. Ho, Y.M. Liu, X.Y. Jing, A.H. Cheng, Synthesis of nano-Fe^0/PEI composite and its reduction and chelation mechanisms for Cr(VI) from aqueous solution, J. Environ. Eng., 144 (2018) 04018004.

[31] S.K. Xian, F. Xu, C. Ma, Y. Wu, Q.B. Xia, H.H. Wang, Z. Li, Vapor-enhanced CO_2 adsorption mechanism of composite PEI@ZIF-8 modified by polyethyleneimine for CO_2/N_2 separation, Chem. Eng. J., 280 (2015) 363–369.

[32] Q.M. Fu, J. Ding, W.L. Wang, J.F. Lu, Q.H. Huang, Carbon dioxide adsorption over amine-functionalized MOFs, Energy Procedia, 142 (2017) 2152–2157.

[33] Y.C. Lin, Q.J. Yan, C.L. Kong, L. Chen, Polyethyleneimine incorporated metal-organic frameworks adsorbent for highly selective CO_2 capture, Sci. Rep., 3 (2013) 1859.

[34] X.P. Quan, Z.Q. Sun, H. Meng, Y.D. Han, J.B. Wu, J.L. Xu, Y. Xu, X. Zhang, Polyethyleneimine (PEI) incorporated Cu-BTC composites: Extended applications in ultra-high efficient removal of Congo red, J. Solid State. Chem., 270 (2019) 231–241.

[35] G. Ferey, C. Mellot-Draznieks, C. Serre, F. Millange, J. Dutour, S. Surble, I. Margiolaki, A chromium terephthalate-based solid with unusually large pore volumes and surface area, Science, 309 (2005) 2040–2042.

[36] S. Pourebrahimi, M. Kazemeini, A kinetic study of facile fabrication of MIL-101(Cr) metal-organic framework: effect of synthetic method, Inorg. Chim. Acta, 471 (2018) 513–520.

[37] S.N. Yu, F.S. Pan, S. Yang, H. Ding, Z.Y. Jiang, B.Y. Wang, Z.X. Li, X.Z. Cao, Enhanced pervaporation performance of MIL-101(Cr) filled polysiloxane hybrid membranes in desulfurization of model gasoline, Chem. Eng. Sci., 135 (2015) 479–488.

[38] Y.X. Gao, K. Liu, R.X. Kang, J. Xia, G. Yu, S.B. Deng, A comparative study of rigid and flexible MOFs for the adsorption of pharmaceuticals: kinetics, isotherms and mechanisms, J. Hazard. Mater., 359 (2018) 248–257.

[39] N.A.A. Qasem, N.U. Qadir, R. Ben-Mansour, S.A.M. Said, Synthesis, characterization, and CO_2 breakthrough adsorption of a novel MWCNT/MIL-101(Cr) composite, J. CO_2 Util., 22 (2017) 238–249.

[40] M.S. Alivand, M. Shafiei-Alavijeh, N.H.M.H. Tehrani, E. Ghasemy, A. Rashidi, S. Fakhraie, Facile and high-yield synthesis of improved MIL-101(Cr) metal-organic framework with exceptional CO_2 and H_2S uptake; the impact of excess ligand-cluster, Microporous Mesoporous Mater., 279 (2019) 153–164.

[41] F.T. Liu, W.J. Xiong, J.Y. Liu, Q. Cheng, G. Cheng, L. Shi, Y.B. Zhang, Novel amino-functionalized carbon material derived from metal organic framework: a characteristic adsorbent for U(VI) removal from aqueous environment, Colloid Surf., A, 556 (2018) 72–80.

[42] Y. Zheng, F.C. Chu, B. Zhang, J. Yan, Y.L. Chen, Ultrahigh adsorption capacities of carbon tetrachloride on MIL-101 and MIL-101/graphene oxide composites, Microporous Mesoporous Mater., 263 (2018) 71–76.

[43] S.S. Sambaza, M.L. Masheane, S.P. Malinga, E.N. Nxumalo, S.D. Mhlanga, Polyethyleneimine-carbon nanotube polymeric nanocomposite adsorbents for the removal of Cr^{6+} from water, Phys. Chem. Earth, 100 (2017) 236–246.

[44] W.Q. Cai, Z.L. Li, J.H. Wei, Y. Liu, Synthesis of peanut shell based magnetic activated carbon with excellent adsorption performance towards electroplating wastewater, Chem. Eng. Res. Des., 140 (2018) 23–32.

[45] S.Q. Liu, Y.Y. Sun, R.L. Wang, S.B. Mishra, H.M. Duan, H. Qu, Modification of sand with iron and copper derived from electroplating wastewater for efficient adsorption of phosphorus from aqueous solutions: a combinatorial approach for an effective waste minimization, J. Cleaner Prod., 200 (2018) 471–477.

[46] S. Azizian, Kinetic Models of Sorption: A Theoretical Analysis, J. Colloid Interface Sci., 276 (2004) 47–52.

[47] N. Sykam, N.D. Jayram, G.M. Rao, Exfoliation of graphite as flexible SERS substrate with high dye adsorption capacity for Rhodamine 6G, Appl. Surf. Sci., 471 (2019) 375–386.

[48] D.Vamvuka, S. Dermitzakis, D. Pentari, S.S. fakiotakis, Valorization of Meat and Bone Meal through pyrolysis for soil amendment or lead adsorption from wastewaters, Food Bioprod. Process., 109 (2018) 148–157.

[49] Q. Liu, Q.Z. Liu, B.S. Liu, T. Hu, W.L. Liu, J.S. Yao, Green synthesis of tannin-hexamethylenediamine based adsorbents for efficient removal of Cr(VI), J. Hazard. Mater., 352 (2018) 27–35.

[50] F. Ogataa, E. Uetaa, N. Kawasaki, Characteristics of a novel adsorbent Fe-Mg-type hydrotalcite and its adsorption capability of As(III) and Cr(VI) from aqueous solution, J. Ind. Eng. Chem., 59 (2018) 56–63.

[51] Z.H. Yang, J. Cao, Y.P. Chen, X. Lia, W.P. Xiong, Y.Y. Zhou, C.Y. Zhou, R. Xu, Y.R. Zhang, Mn-doped zirconium metal-organic framework as an effective adsorbent for removal of tetracycline and Cr(VI) from aqueous solution, Microporous Mesoporous Mater., 277 (2019) 277–285.

[52] S. Saini, S. Arora, Kirandeep, B.P. Singh, J.K. Katnoria, I. Kaur, Nitrilotriacetic acid modified bamboo charcoal (NTA-MBC): an effective adsorbent for the removal of Cr (III) and Cr (VI) from aqueous solution, J. Environ. Chem. Eng., 6 (2018) 2965–2974.

[53] Q.P. Kong, J.Y. Wei, Y. Hu, C.H. Wei, Fabrication of terminal amino hyperbranched polymer modified graphene oxide and its prominent adsorption performance towards Cr(VI), J. Hazard. Mater., 363 (2019) 161–169.

[54] H.T.M. Thanh, T.T.T. Phuong, P.T.L. Hang, T.T.T. Toan, T.N.T., T.X. Mau, D.Q. Khieu, Comparative study of Pb(II) adsorption onto MIL-101 and Fe-MIL-101 from aqueous solutions, J. Environ. Chem. Eng., 6 (2018) 4093–4102.

[55] M. Chairat, S. Rattanaphani, J.B. Bremner, V. Rattanaphani, Adsorption kinetic study of lac dyeing on cotton, Dyes Pigm., 76 (2008) 435–439.